

On the Cause and Control of Residual Voltage Generated by Electrical Stimulation of Neural Tissue

Ashwati Krishnan¹ and Shawn K. Kelly², *Member, IEEE*

Abstract—Functional electrical stimulation of neural tissue is traditionally performed with symmetric cathodic-first biphasic pulses of current through an electrode/electrolyte interface. When the interface is modeled by a series R-C circuit, as is sometimes done for stimulator circuit design, the appearance of a net residual voltage across the electrode cannot be explained. Residual voltage can cause polarization of the electrode and pose a problem for safe electrical stimulation. This paper aims to (1) theoretically explain one reason for the residual voltage, which is the inclusion of the Faradaic impedance (2) suggest a simple dynamic feedback mechanism to eliminate residual voltage.

I. INTRODUCTION

Physiological experiments on neural tissue have shown that electrical stimulation of excitable cells can evoke functional responses [1]. Numerous artificial prosthetic devices are based on electrical stimulation of tissue with an electrode. Electrical stimulation of tissue is usually realized by delivering a series of controlled biphasic, charge-balanced current pulses through an electrode/tissue interface [2]. A biphasic waveform consists of a cathodic pulse of current, followed by an anodic pulse of current to neutralize the total charge delivered to the tissue (Fig. 1). Neural tissue is stimulated by driving a cathodic-first biphasic current signal, because less current is required to depolarize the cell [3]. There also exist limitations on the geometric charge density as well as the amount of charge per phase that can be delivered without causing damage to the tissue [4].

When a metal electrode is placed in an electrolyte, current flow is determined by the flow of electrons through the metal electrode and the flow of ions through the electrolyte [3]. Due to the presence of a double layer of charge at the electrode, the main component of the electrode/electrolyte interface model is a capacitor, C [5]. The resistance of the electrolyte, combined with resistance due to wires and contacts is modeled as a spreading (series) resistance, R_s . Oxidation-reduction reactions at the electrode/electrolyte interface give rise to current flow that is modeled by a charge-transfer resistance R_{ct} . The mass transport limitations of ions in the electrolyte is modeled by the *Warburg* impedance [6]. Together, the charge-

transfer resistance and Warburg impedance can be lumped as a Faradaic impedance [3].

A high impedance current source is required to deliver charge to the tissue through an electrode. The circuit is completed by using a return electrode placed in the vicinity of the same electrode-tissue interface. The design of a practical current source requires an electrical load model that best represents the behavior of the electrode-tissue interface. A first-order model commonly used to represent the electrode/electrolyte interface is that of a series R-C [5]. The use of a series R-C model leads to a misconception that a charge-balanced biphasic stimulus to an electrode/electrolyte interface results in a zero net voltage. However there exists a net residual voltage at the end of the anodic pulse, even if the biphasic stimulus is completely charge balanced [7]. The residual voltage is due to the Faradaic impedance [6] as well as mismatch errors in the transistors used to make the stimulator. The presence of a residual voltage may lead to irreversible chemical reactions at the electrode-tissue interface and cause tissue damage [8]. In order to overcome this residual voltage, two popular methods currently exist. The first method is the connection of a large DC blocking capacitor in series with the stimulating electrode [9]. A large capacitor tends to take a lot of die area for an implantable integrated circuit, and is not preferred, especially for large multielectrode arrays [8]. The second is to short the electrode to ground [10] after the anodic pulse. Shorting switches can cause current spikes and lead to an uncontrolled discharge process [11]. Moreover, relying on only one mechanism to prevent electrode/tissue damage in a medical device meant for chronic use, is a precarious approach. This paper proposes a feedback sense-and-control mechanism to dynamically control the residual voltage of an electrode stimulated by biphasic current.

II. THEORY

A commonly used model for the electrode-tissue interface for a stimulator is the series R-C model (Fig. 2(a)). The effect of the charge-transfer resistance, R_{ct} and the Warburg impedance has been modeled as a Faradaic resistance, R_w , in parallel with the double layer capacitance, C . The resulting circuit is known as Randles R-C-R model (Fig. 2(b)) [3]. Charge build-up on the electrode (which results in a net residual voltage) is often attributed to mismatch errors in charge-balanced waveforms due to process variations in integrated circuit manufacturing technology [12], [13], [8], but is not the only cause for residual voltage. The transient output voltage for a typical biphasic current stimulus has been derived

*Research supported in part by the Department of Veterans Affairs Center for Innovative Visual Rehabilitation (VA CIVR) and the Institute for Complex Engineered Systems, Carnegie Mellon University. MOSIS provides in-kind foundry services.

¹Ashwati Krishnan is with the Department of Electrical and Computer Engineering and the Institute of Complex Engineered Systems (ICES), Carnegie Mellon University, Pittsburgh, PA 15213, USA. Email: ashwatic@andrew.cmu.edu

²Shawn K. Kelly is with the VA CIVR, Boston, MA 02130, USA, and with the Institute of Complex Engineered Systems, Carnegie Mellon University, Pittsburgh, PA 15213, USA. Email: skkelly@cmu.edu

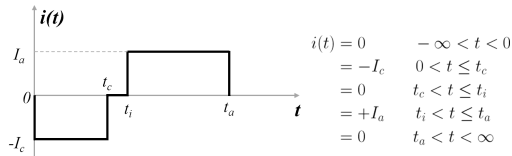


Fig. 1. Typical biphasic stimulation current signal

to illustrate the theoretical existence of a non-zero residual voltage due to R_w .

A. Input Signal

Consider the cathodic biphasic current signal shown in Fig. 1. The transient equation of the current is given by:

$$i(t) = -I_c[u(t) - u(t - t_c)] + I_a[u(t - t_i) - u(t - t_a)], \quad (1)$$

where I_c, I_a are the cathodic/anodic amplitudes, t_c, t_i, t_a are the end of the cathodic pulse, interphase delay, anodic pulse respectively.

B. R-C Model

A first order R-C series model is shown in Fig. 2(a).

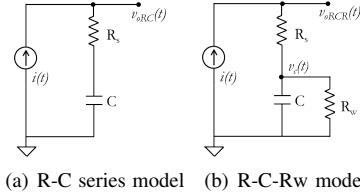


Fig. 2. An ideal piecewise linear current source driving the biphasic stimulus pulse through a (a) R-C model (b) R-C-R model of an electrode/electrolyte interface. R_s is the (spreading) resistance of the electrolyte, C represents the double-layer capacitance and R_w is the parallel Faradaic resistance that models the charge-transfer resistance, R_{ct} and the Warburg impedance.

The output voltage $v_{oRC}(t)$ is given by:

$$v_{oRC}(t) = [R_s + \frac{t}{C}]i(t) - u(t - t_c)\frac{I_c t_c}{C} - u(t - t_i)\frac{I_a t_i}{C} + u(t - t_a)\frac{I_a t_a}{C}. \quad (2)$$

Biphasic signals can be symmetric or asymmetric [14]. In particular, the residual output voltage when the pulses are symmetric and charge balanced, e.g., $I_a = I_c = I$; $(t_c - 0) = (t_a - t_i)$, is given by:

$$v_{oRC}(t_a^+) = 0. \quad (3)$$

C. R-C-R Model

The same analysis is performed on a second order R-C-R model shown in Fig. 2(b). An insight into the physical interpretation of the Warburg impedance can be found in [6]. However, for the purposes of this design, the parallel Faradaic impedance has been modeled here as a linear resistor. The output voltage $v_{oRCR}(t)$ is given by:

$$v_{oRCR}(t) = (R_s + R_w) \cdot i(t) - R_w \left[(-I_c)[u(t)e^{-\frac{t}{\tau}} - u(t - t_c)e^{-\frac{(t-t_c)}{\tau}}] + I_a \left[u(t - t_i)e^{-\frac{(t-t_i)}{\tau}} - u(t - t_a)e^{-\frac{(t-t_a)}{\tau}} \right] \right]. \quad (4)$$

In this case, the residual output voltage when the pulses are charge balanced, is,

$$v_{oRCR}(t_a^+) = IR_w \left[1 + e^{-\frac{t_a}{\tau}} - e^{-\frac{(t_a-t_c)}{\tau}} - e^{-\frac{(t_a-t_i)}{\tau}} \right]. \quad (5)$$

By comparing (3) and (5), it can be seen that there exists a theoretical non-zero residual voltage due to the inclusion of the resistance, R_w , in the standard electrode model. Intuitively, in the R-C model, the capacitor does not have a discharge path through which it can leak current, which it does in the R-C-R model. The derived expression shows that for a first-order assumption of the Faradaic impedance, a symmetric charge balanced waveform can result in a residual voltage on the electrode.

III. METHODS

A. Biphasic Stimulator Circuit

A simple dual-supply biphasic stimulator circuit was constructed using off-the-shelf components to generate cathodic-first biphasic current pulses of $100 \mu\text{A}$, for 1 ms per phase. The stimulus pulse was driven at 100 Hz. Bipolar junction transistors were biased with voltage dividers to establish the required current. A microcontroller was used to control the timing of the currents (via MOSFET switches). The stimulator circuit is shown in Fig. 3.

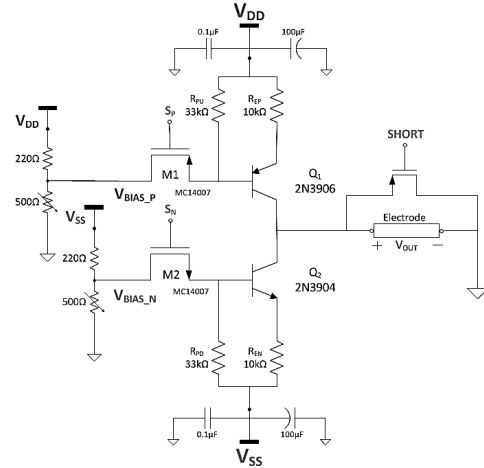


Fig. 3. Bench-top biphasic stimulator

The voltage, V_{OUT} , across the stimulation electrode was measured at the end of the anodic pulse by an inverting sample-and-hold amplifier (Fig. 4) and is denoted as the residual voltage, V_{RES} . A bias voltage, V_{MID} , was applied to ensure that a negative electrode voltage could be fed into the analog-to-digital converter (ADC) of the microcontroller. The complete system setup is shown in Fig. 5 and the timing diagram for the control signals is shown in Fig. 6.

A major limitation in the bench-top biphasic stimulator design was the DC bias error due to the mismatch in the commercial NPN and PNP bipolar transistors that were used in the circuit. The drift in voltage due to charge build-up by the DC bias was slower than the rate of stimulation. A switch

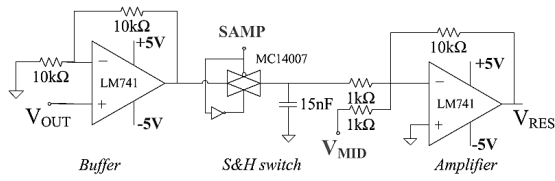


Fig. 4. Sample-and-hold amplifier

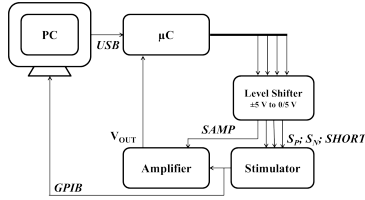


Fig. 5. Bench setup system schematic

was used to short the electrode to ground when it was not being stimulated. An integrated circuit stimulator will be less prone to this DC bias, when compared to a bench-top circuit.

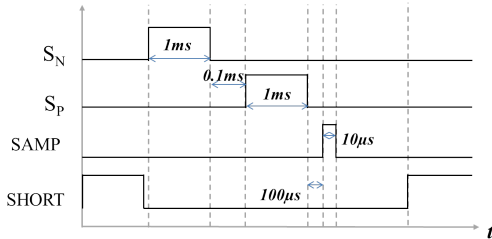


Fig. 6. Timing diagram for biphasic stimulator with feedback. S_N and S_P are signals that run on the cathodic and anodic pulses. $SAMP$ samples the output residual voltage. $SHORT$ shorts out the stimulation electrode when not in use.

B. Feedback

A mechanism to control the residual voltage using charge-balancing pulses has been proposed in [11]. In order to control the residual voltage, a dynamic alteration of anodic pulse width is proposed such that the resulting voltage is nulled and controlled. The output voltage at the end of the anodic pulse was sampled and sent to a proportional feedback controller, implemented in software by the microcontroller. The calculated width of the instantaneous anodic pulse is,

$$t_{pulse-up}[n+1] = t_{pulse-up}[n] - k(V_{OUT}[n] - V_{SP}), \quad (6)$$

where k is the proportional feedback parameter. The set point voltage (V_{SP}) was 0 V and the value of k was selected to be high enough to provide feedback and not induce oscillations in the system. A transient experiment was performed in which the value of feedback gain was changed after 10 s from $k = 0$ s/V to $k=1000$ s/V.

C. Electrode Modeling

The bench-top experiments on the electrode/electrolyte impedance were performed in saline solution. The electrodes are 400 μm in diameter, made of sputtered iridium oxide film (SIROF) and were obtained as part of the Boston Retinal Implant Project [15]. These electrodes have been used to stimulate retinal neurons in visual prosthesis devices. Fabrication and structural details of the electrode can be found in [15].

The return electrode was a 0.5cm exposed 22AWG wire (with a tin-plated copper core) placed in the same saline solution. The electrodes were driven using the biphasic stimulator setup described in Section III-A. The parameters of the R-C-R model of the electrode/saline interface were obtained by performing a model fit on a step-response voltage output to the model derived in Section II. An approximate step response for the electrode was obtained using a 5 ms anodic-first biphasic symmetric current pulse (with a time constant of 1 μs). An infinite step response is not possible because that would damage of the electrode due to excessive charge injection. The maximum charge injection capacity of SIROF electrodes is 5 mC/cm^2 [7]. The output voltage across the electrode was measured using an oscilloscope, which was connected to a LabVIEW GPIB interface. A typical waveform is shown in Fig. 7.

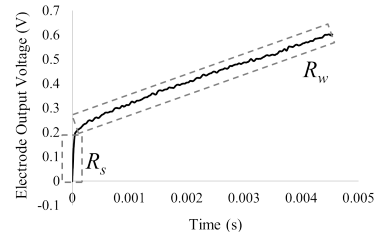


Fig. 7. Step response of an electrode to an anodic pulse. Data used to extract R_s and R_w are highlighted.

The value of step current used was 100 μA . The spreading resistance R_s in saline was extracted by calculating the slope of the initial rise in the output voltage. The value of R_w was obtained by performing non-linear least squares curve fit in MATLAB with the model equation that represents the voltage across the $C - R_w$ circuit,

$$v_{out} = R_w i(t) + A \cdot e^{-\frac{t}{\tau}}. \quad (7)$$

The details of the parameters and the fit are given in Table I. Because the experiments were performed in saline, the value obtained for the spreading resistance, R_s , is typically lower than *in vivo*. The detail of the curve fitting is shown in Fig. 8.

TABLE I
ELECTRODE/SALINE INTERFACE MODEL PARAMETERS

Parameter	R_w	R_s	A	τ	C
Value	17.12 k Ω	2.1k Ω	-1.488 V	15.46 ms	909nF

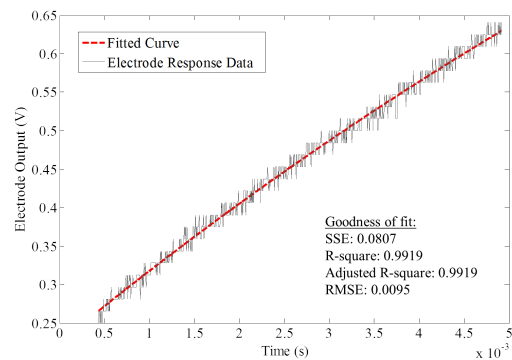


Fig. 8. Comparison of curve fitting result with experimental data

IV. RESULTS

The residual voltage was measured 2 ms after the end of the anodic pulse and the measurement window spanned 10 μ s. The electrode response is shown in Fig. 9, superimposed over the sampling signal.

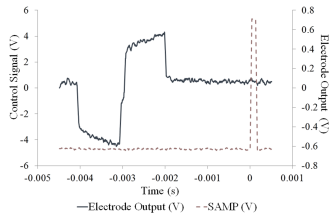


Fig. 9. Output voltage in response to a symmetric biphasic current signal for a SIROF electrode in saline. The sampling signal from the controller shown measures the residual voltage 2ms after the anodic pulse.

The feedback was enforced at $t = 10$ s by setting $k = 1000$ s/V from $k = 0$ s/V (Fig. 10). Fine-tuning of the proportionality constant was not pursued.

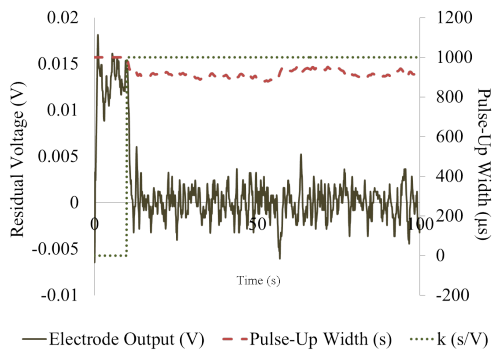


Fig. 10. Effect of feedback on the residual voltage at the end of a biphasic stimulus pulse.

Region A in Fig. 10 indicates the residual voltage that exists on the electrode without feedback. The width of the anodic pulse remains unaltered during this time. Region B clearly shows that the residual voltage is being maintained at the set point ($V_{SP} = 0$), due to the onset of the feedback set by $k = 1000$ s/V. The average anodic pulse width is about 916 μ s because the residual voltage is positive.

V. CONCLUSION & FUTURE WORK

This paper presents an analytical study on the effect of a parallel Faradaic impedance on the residual voltage of an electrically stimulated electrode, and not just due to transistor mismatch errors. The value of the modeled impedance varies largely due to the electrode/electrolyte interface, and explains the existence of a net residual voltage. The existence of a residual voltage can cause damage to the electrode through irreversible chemical reactions in the long term [16]. Therefore, there is a necessity to reduce this voltage, rather than maintain charge-balance. Simple bench-top experiments in saline have shown that an active feedback mechanism can help reduce the net residual voltage to zero, regardless of the origin of the voltage. The main objective of this proof-of-concept paper is

to show that the residual voltage can be controlled by adjusting the width of the anodic pulse.

There is a need to further study the chronic effects of the residual voltage *in vivo*. The subsequent step is to characterize the effect of feedback on an electrode by implementing an application-specific integrated circuit (ASIC), so that transistor mismatch errors (as compared to off-the-shelf components) are minimized. ASIC stimulators also provide the opportunity to quantify the contribution of the Faradaic impedance to the residual voltage, as well as explore more complex feedback algorithms *in vivo*.

ACKNOWLEDGMENT

The authors would like to thank Dr. Gary Fedder (Institute of Complex Engineered Systems at Carnegie Mellon University) for his advice and support, as well as the ECE Department and the members of the MEMS Lab for providing support, resources and equipment.

REFERENCES

- [1] E. J. Tehovnik, "Electrical stimulation of neural tissue to evoke behavioral responses." *Journal of Neuroscience Methods*, vol. 65, no. 1, pp. 1–17, Mar. 1996.
- [2] J. C. Lilly *et al.*, *Science*, vol. 121, pp. 468–469, 1955.
- [3] D. R. Merrill, *The Electrochemistry of Charge Injection at the Electrode/Tissue Interface*, D. D. Zhou and E. Greebaum, Eds. Springer, 2010.
- [4] D. B. McCreery, W. F. Agnew, T. G. Yuen, and L. Bullara, "Charge density and charge per phase as cofactors in neural injury induced by electrical stimulation," *IEEE Transactions on Biomedical Engineering*, vol. 37, pp. 996–1001, 1990.
- [5] L. A. Geddes, "Historical evolution of circuit models for the electrode-electrolyte interface," *Annals of Biomedical Engineering*, vol. 25.
- [6] S. R. Taylor and E. Gileadi, "Physical interpretation of the warburg impedance," *Corrosion Science*, vol. 51.
- [7] S. F. Cogan, "Neural stimulation and recording electrodes," *Annual Review of Biomedical Engineering*, vol. 10, pp. 275–309, 2008.
- [8] M. Ortmanns, "Charge balancing in functional electrical stimulators: A comparative study," *IEEE International Symposium on Circuits and Systems*, pp. 573 – 576, 2007.
- [9] J. Patrick, P. Seligman, D. Money, and J. Kuzma, "Engineering, in cochlear prosthesis," *IEEE Engineering in Medicine and Biology Magazine*, vol. 6, pp. 42–46, 1987.
- [10] R. White, "System design of a cochlear implant," *IEEE Engineering in Medicine and Biology Magazine*, vol. 6, pp. 42–46, 1987.
- [11] K. Sooksood, T. Stieglitz, and M. Ortmanns, "An active approach for charge balancing in functional electrical stimulation," *IEEE Transactions on Biomedical Circuits and Systems*, vol. 4, pp. 162 – 170, 2010.
- [12] J.-J. Sit and R. Sarpeshkar, "A low-power blocking-capacitor-free with less than 6 na dc error for 1-ma," *IEEE Transactions on Biomedical Circuits and Systems*, vol. 1, pp. 172–183, 2007.
- [13] M. Sivaprakasam, W. Liu, M. S. Humayun, and J. D. Weiland, "A variable range bi-phasic current stimulus driver circuitry for an implantable retinal prosthetic device," *IEEE Journal of Solid State Circuits*, vol. 40, pp. 763–771, 2005.
- [14] S. F. Cogan *et al.*, "Potential-biased, asymmetric waveforms for charge-injection with activated iridium oxide (airof) neural stimulation electrodes," *IEEE Transactions on Biomedical Engineering*, vol. 53, pp. 327 – 332, 2006.
- [15] D. B. Shire *et al.*, "Development and implantation of a minimally invasive wireless subretinal neurostimulator," *IEEE Transactions on Biomedical Engineering*, vol. 56, pp. 2502–2511, 2009.
- [16] A. Scheiner, J. T. Mortimer, and U. Roessmann, "Imbalanced biphasic electrical stimulation: Muscle tissue damage," *Annual International Conference of the IEEE Engineering in Medicine and Biology Society*, vol. 12, pp. 1486 – 1487, 1990.